Relativistic Measurement Backaction in the Quantum Dirac Oscillator

Keye Zhang,[1,4,*] Lu Zhou,[1,4] Pierre Meystre,[2] and Weiping Zhang[3,4,†]
[1]Quantum Institute for Light and Atoms, School of Physics and Material Science, East China Normal University, Shanghai 200241, People's Republic of China
[2]Department of Physics and College of Optical Sciences, University of Arizona, Tucson, Arizona 85721, USA
[3]Department of Physics and Astronomy, Shanghai Jiao Tong University, and Tsung-Dao Lee Institute, Shanghai 200240, China
[4]Collaborative Innovation Center of Extreme Optics, Shanxi University, Taiyuan, Shanxi 030006, People's Republic of China

(Received 9 July 2018; revised manuscript received 15 August 2018; published 11 September 2018)

An elegant method to circumvent quantum measurement backaction is the use of quantum mechanics free subsystems (QMFS), with one approach involving the use of two oscillators with effective masses of opposite signs. Since negative energies, and hence masses, are a characteristic of relativistic systems a natural question is to what extent QMFS can be realized in this context. Using the example of a one-dimensional Dirac oscillator we investigate conditions under which this can be achieved, and identify *Zitterbewegung* or virtual pair creation as the physical mechanism that fundamentally limits the feasibility of the scheme. We propose a tabletop implementation of a Dirac oscillator system based on a spin-orbit coupled ultracold atomic sample that allows for a direct observation of the corresponding analog of virtual pair creation on quantum measurement backaction.

DOI: 10.1103/PhysRevLett.121.110401

Introduction.—A major challenge of quantum metrology is the need to minimize the backaction noise that accompanies the measurement of quantum observables. Efforts at circumventing this difficulty have led to the development of quantum nondemolition measurements, and to the use of nonclassical field states that locate quantum fluctuations where they do not significantly perturb the measurement. More recently, Tsang and Caves [1] and Polzik and coworkers [2] realized that it is sometimes possible to isolate quantum-mechanics free subsystems (QMFS) of a quantum system whose observables are by construction quantum nondemolition observables.

An example considered in Ref. [1] consists of two harmonic oscillators of identical frequencies and opposite masses described by the Hamiltonian

$$H = \frac{\hat{p}^2}{2m} + \frac{1}{2}m\omega^2\hat{x}^2 - \frac{\hat{p}'^2}{2m} - \frac{1}{2}m\omega^2\hat{x}'^2. \tag{1}$$

Considering the composite variables $\hat{X} = \hat{x} + \hat{x}'$, $\hat{P} = \frac{1}{2}(\hat{p} + \hat{p}')$, $\hat{\Phi} = \frac{1}{2}(\hat{x} - \hat{x}')$, and $\hat{\Pi} = \hat{p} - \hat{p}'$, with $[\hat{X}, \hat{\Pi}] = [\hat{P}, \hat{\Phi}] = 0$, it is easily verified that the Heisenberg equations of motion for $\hat{X}$ and $\hat{\Pi}$ form the closed system

$$\dot{\hat{X}}(t) = \frac{\hat{\Pi}(t)}{m}, \qquad \dot{\hat{\Pi}} = -m\omega^2\hat{X}(t), \tag{2}$$

so that $\hat{X}$ and $\hat{\Pi}$, the collective position and relative momentum, form a QMFS that allows for their simultaneous and repeated measurement with arbitrary accuracy—and likewise for the pair $\{\hat{\Phi}, \hat{P}\}$. QMFS implementations have been realized in atomic spin ensembles [3], hybrid optomechanical systems [4], microwave-coupled mechanical oscillators [5], and have been proposed in Bose-Einstein condensates with negative effective mass component [6].

The fact that the QMFS of Ref. [1] relies on the use of a negative mass oscillator leads one to ask to what extent the negative energy states in relativistic quantum systems can result in the existence of QMFS in these systems as well. This is the question that we address, using the example of a one-dimensional Dirac oscillator. We find that already in that implementation it is fundamentally different from two independent harmonic oscillators of opposite masses, due to the presence of a "spin-orbit" couplinglike term associated with relativistic *Zitterbewegung*: even in the nonrelativistic limit its remnants limit the ability to realize backaction evading measurements—this is in addition to the known fact that the localization of particles is limited by the Compton wavelength λ_c. We then quantify the impact of *Zitterbewegung* in the full relativistic regime. We conclude by proposing a tabletop atomic, molecular, and optical physics implementation that permits us to demonstrate this behavior in a nonrelativistic system.

Model.—The Dirac oscillator is an extension of the Dirac equation for a free particle that is linear both in position and momentum. It was introduced by Moshinsky *et al.* [7], who added the linear vector potential $-i\beta m\omega\hat{x}$ to the Dirac equation. In addition to its use in nuclear physics and relativistic quantum physics, see, e.g., the reviews [8,9], it has found applications in fields ranging from condensed matter physics to quantum optics [10–13].

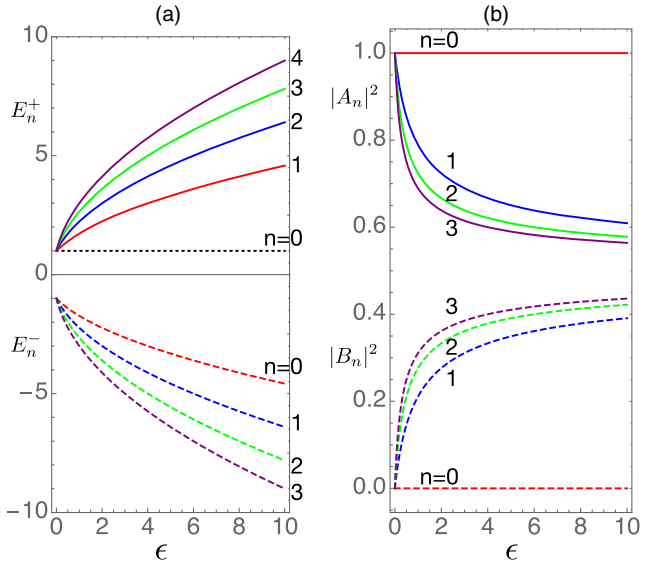

FIG. 1. (a) Eigenenergies $E_n^{\pm}$, $n = 0, \ldots, 4$, in units of mc^2 as a function of the ratio $\varepsilon = \hbar\omega/mc^2$. (b) Probabilities $|A_n|^2$ and $|B_n|^2$, $n = 0, \ldots, 3$, of the two components of the eigenstates.

We concentrate on one spatial dimension, in which case the Dirac matrices α and β reduce to the Pauli operators $\hat{\sigma}_x$ and $\hat{\sigma}_z$, leading to the reduced equation

$$i\hbar\partial_t|\Psi\rangle = [c\hat{\sigma}_x\hat{p} - mc\omega\hat{\sigma}_y\hat{x} + mc^2\hat{\sigma}_z]|\Psi\rangle \equiv H_{\rm DO}|\Psi\rangle. \quad (3)$$

The energy spectrum of $H_{\rm DO}$ comprises a positive energy branch with eigenenergies $E_n^+ = mc^2\sqrt{1 + 2n\hbar\omega/mc^2}$ bounded from below by mc^2 and a negative energy branch with energies $E_n^- = -E_{n+1}^+$ bounded from above by $-mc^2\sqrt{1 + 2\hbar\omega/mc^2}$, see Fig. 1(a).

The corresponding eigenstates are $|E_n^+\rangle = A_n|n,\uparrow\rangle - iB_n|n-1,\downarrow\rangle$ and $|E_n^-\rangle = B_{n+1}|n+1,\uparrow\rangle + iA_{n+1}|n,\downarrow\rangle$, where $|n\rangle$ are the eigenstates of a nonrelativistic harmonic oscillator, $|\uparrow,\downarrow\rangle$ are Pauli spinors, and $A_n = \sqrt{(E_n^+ + mc^2)/2E_n^+}$ and $B_n = \sqrt{(E_n^+ - mc^2)/2E_n^+}$. The fact that the eigenstates of the Dirac oscillator are linear superpositions of the motional and spin states $|n,\uparrow\rangle$ and $|n-1,\downarrow\rangle$ is a consequence of the spin-orbit coupling interaction in $H_{\rm DO}$, a relativistic effect resulting from enforcing first-order spatial dependences in its wave equation.

Figure 1(b) plots $|A_n|^2$ and $|B_n|^2$ for $n = 0, \ldots, 3$ as a function of the relativistic parameter $\varepsilon \equiv \hbar\omega/mc^2$. For $\varepsilon \gg 1$, we have that $|A_n| \approx |B_n| \approx 1/\sqrt{2}$, and the eigenstates $|E_n^{\pm}\rangle$ exhibit spin-orbit coupling and entanglement between motional and spin degree of freedom. In the nonrelativistic limit $\varepsilon \to 0$, in contrast, $|A_n| \to 1$ and $|B_n| \to 0$, and the eigenstates and eigenenergies reduce to those of two harmonic oscillators of frequency ω associated with the spin-up and spin-down components. The first one has a positive mass m and ground state energy mc^2, and the second one a negative mass $-m$ and energy bound from above by $-(\hbar\omega + mc^2)$.

Nonrelativistic limit.—For $\varepsilon \to 0$ the Dirac oscillator can, therefore, be approximated by the Hamiltonian

$$H_{\rm nr} = \left(mc^2 + \frac{\hat{p}^2}{2m} + \frac{m\omega^2\hat{x}^2}{2}\right)\hat{\sigma}_z - \frac{\hbar\omega}{2}, \quad (4)$$

which describes a pair of one-dimensional harmonic oscillators of spin-dependent mass—positive mass for spin up and negative mass for spin down. While this suggests that it might be possible to form a QMFS similar to that of Ref. [1] there is an important difference between the Hamiltonians (4) and (1), the seemingly inconsequential spin operator $\hat{\sigma}_z$, the remnant of the spin-orbit coupling. We see shortly that it results in profound differences in the dynamics of the two systems.

In analogy with Ref. [1] we introduce the operators $\hat{X} = \hat{x}I = \hat{x}|\uparrow\rangle\langle\uparrow| + \hat{x}|\downarrow\rangle\langle\downarrow| \equiv \hat{x}_\uparrow + \hat{x}_\downarrow$ and $\hat{\Pi} = \hat{p}\hat{\sigma}_z = \hat{p}|\uparrow\rangle\langle\uparrow| - \hat{p}|\downarrow\rangle\langle\downarrow| \equiv \hat{p}_\uparrow - \hat{p}_\downarrow$ which satisfy the closed set of Heisenberg equations of motion (2), with, however, the important difference that $[\hat{X},\hat{\Pi}] = i\hbar\hat{\sigma}_z$, instead of $[\hat{X},\hat{\Pi}] = 0$. The associated Heisenberg uncertainty relation is, therefore, $\Delta\hat{X}\Delta\hat{\Pi} \geq (\hbar/2)|\langle\hat{\sigma}_z\rangle|$.

One might expect that since $\hat{X}$ and $\hat{\Pi}$ commute for $\langle\hat{\sigma}_z\rangle \to 0$ they would form a QMFS in that limit, with an analogous QMFS for the pair of operators $\hat{P} \equiv \hat{p}I$ and $\hat{\Phi} \equiv \hat{x}\hat{\sigma}_z$. This is, however, not correct, due to the fact that these are *composite* observables of the center-of-mass and spin degrees of freedom. While $\hat{X}$ has a same expectation value as the center-of-mass position $\hat{x}$, $\langle\hat{\Pi}\rangle$ normally differs from $\langle\hat{p}\rangle$, and can, in particular, be different from zero even for $\langle\hat{\sigma}_z\rangle = 0$. More importantly, since $\hat{\sigma}_z^2 = I$ we have $\hat{X}^2 = \hat{\Phi}^2$ and $\hat{P}^2 = \hat{\Pi}^2$, so that the separation of the dynamics into two independent dynamical subsystems is invalid for the high-order moments of $\{\hat{X},\hat{\Pi}\}$ and $\{\hat{\Phi},\hat{P}\}$. As a result, measurement backaction, while not affecting the evolution of $\langle\hat{X}\rangle$ and $\langle\hat{\Pi}\rangle$ for $\langle\hat{\sigma}_z\rangle = 0$, does impact their fluctuations, rendering a backaction evading sequence of measurements impossible.

As a concrete example, we consider using a Dirac oscillator operating in the nonrelativistic limit $\varepsilon \to 0$ to perform measurements of a weak spin-dependent external perturbation of the form $V_f = f\hat{\sigma}_z$ by imprinting its position $\hat{x}$ on the phase of a quantum harmonic oscillator, the measuring apparatus. The Hamiltonian describing this measurement scheme is

$$H_{\rm total} = H_{\rm nr} + \hbar\omega_b\hat{b}^\dagger\hat{b} + (g\hat{b}^\dagger\hat{b} + f\hat{\sigma}_z)\hat{x}, \quad (5)$$

where $b^\dagger$ and $\hat{b}$ are the creation and annihilation operators of the measuring oscillator, and g a coupling constant. In the nonrelativistic limit $d\hat{\sigma}_z/dt \to 0$ the Heisenberg equations of motion reduce to

$$\frac{d\hat{X}}{dt} = \hat{\sigma}_z \frac{\hat{p}}{m} = \frac{\hat{\Pi}}{m}, \qquad \frac{d\hat{b}}{dt} = -i\left(\omega_b + \frac{g}{\hbar}\hat{X}\right)\hat{b},$$
$$\frac{d\hat{\Pi}}{dt} = \hat{\sigma}_z \frac{d\hat{p}}{dt} = -m\omega^2\hat{X} - g\hat{b}^\dagger\hat{b}\hat{\sigma}_z - f, \tag{6}$$

where $-g\hat{b}^\dagger\hat{b}\hat{\sigma}_z$ accounts for measurement backaction [14]. Solving these equations for $\hat{X}(t)$ gives

$$\hat{X}(t) = \hat{X}(t_0)\cos\omega t + \frac{\hat{\Pi}(t_0)}{m\omega}\sin\omega t - \frac{2(f + g\hat{b}^\dagger\hat{b}\hat{\sigma}_z)}{m\omega^2}\sin^2\frac{\omega t}{2}. \tag{7}$$

This confirms that for $\langle\hat{\sigma}_z\rangle \to 0$ and initially uncorrelated system and measurement apparatus, $\langle\hat{b}^\dagger\hat{b}\hat{\sigma}_z\rangle = \langle\hat{b}^\dagger\hat{b}\rangle\langle\hat{\sigma}_z\rangle$, the measurement of f does not impact the subsequent evolution of $\langle\hat{X}(t)\rangle$. In particular, for $|\Psi_n(0)\rangle = (|n,\uparrow\rangle + |n-1,\downarrow\rangle)/\sqrt{2}$, a superposition that comprises two components of opposite energies and for which $\langle\hat{\sigma}_z\rangle = 0$, this expression reduces to

$$\langle\hat{X}(t)\rangle = -\frac{2f}{m\omega^2}\sin^2\frac{\omega t}{2}, \tag{8}$$

independent of any influence from the measuring apparatus. However, its standard deviation is $\Delta\hat{X} = \sqrt{\langle\hat{X}^2\rangle - \langle\hat{X}\rangle^2} = x_{\mathrm{zpt}}\sqrt{2n + 8G^2\sin^4(\omega t/2)}$, where $G = \sqrt{2}g\langle\hat{b}^\dagger\hat{b}\rangle x_{\mathrm{zpt}}/\hbar\omega$ is a dimensionless measurement strength and $x_{\mathrm{zpt}} = \sqrt{\hbar/2m\omega}$ is the zero-point width of the oscillator wave function. In addition to the n-dependent position uncertainty stemming from the initial state, $\Delta\hat{X}$ comprises a contribution proportional to G, illustrating how measurement backaction limits the precision of subsequent measurements of f.

Relativistic backaction.—Moving past the nonrelativistic limit the anharmonicity and spin-orbit coupling of the Dirac oscillator increasingly prevent the conservation of $\langle\hat{\sigma}_z\rangle$, and measurements disturb not just the higher moments of $\hat{X}$, but $\langle\hat{X}(t)\rangle$ as well. Specifically, the spin-orbit coupling generates *Zitterbewegung* oscillations between the positive and negative energy states of the oscillator, and hence of $\langle\hat{\sigma}_z\rangle$, at a frequency Ω_{zb} of the order of $2mc^2/\hbar$.

For small enough ε one can evaluate $\hat{\sigma}_z(t)$ perturbatively as $\langle\hat{\sigma}_z(t)\rangle \approx \sqrt{2n\varepsilon}\sin(2mc^2t/\hbar)$, see Supplemental Material [15], and

$$\langle\hat{X}(t)\rangle \approx -\frac{2[f + \sqrt{2n\varepsilon}g\langle\hat{b}^\dagger\hat{b}\rangle\sin(2mc^2t/\hbar)]}{m\omega^2}\sin^2\frac{\omega t}{2}. \tag{9}$$

It is characterized by fast *Zitterbewegung* oscillations of small amplitude superposed to slow oscillations at frequency $\omega \ll \Omega_{\mathrm{zb}}$ and of amplitude proportional to $2f$, essentially still given by Eq. (8). Detecting a signal at the bare frequency of the oscillator results, therefore, in an effective smearing $f \pm \Delta$ of the measured force, with $\Delta = \sqrt{2n\varepsilon}g\langle\hat{b}^\dagger\hat{b}\rangle$. Since the amplitude of the *Zitterbewegung* oscillations increases with G the smearing of f can be thought of as a backaction effect that imposes a fundamental limit to the precision of the measurement of f [15]. Alternatively, one can also think of Δ as an indirect probe of virtual pair creation [18].

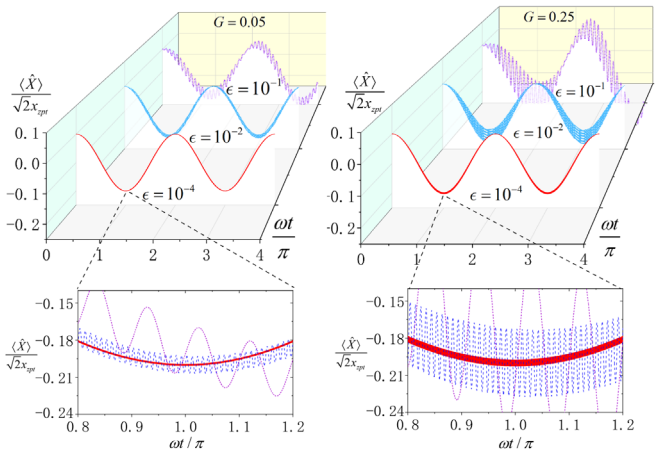

FIG. 2. Time evolution of the dimensionless position $\langle\hat{X}(t)\rangle/\sqrt{2}x_{\mathrm{zpt}}$ for a perturbation amplitude $f = 0.1$, in units of $\hbar\omega/\sqrt{2}x_{\mathrm{zpt}}$, and for increasing relativistic parameters $\varepsilon = 10^{-4}$ (red), 10^{-2} (blue), and 10^{-1} (purple), under the dimensionless measurement strengths $G = \sqrt{2}g\langle\hat{b}^\dagger\hat{b}\rangle x_{\mathrm{zpt}}/\hbar\omega = 0.05$ (left) and 0.25 (right). The lower plots show its detailed evolution near the time $\omega t = \pi$.

Measurement backaction increases with ε, and the frequency difference between ω and Ω_{zb} eventually becomes sufficiently small that $\langle\hat{X}(t)\rangle$ undergoes anharmonic and aperiodic oscillations. This is illustrated in Fig. 2, which shows numerical simulations of $\langle\hat{X}(t)\rangle$ for the initial state $|\Psi_n(0)\rangle$, three values of ε, and two values of G.

We note that in the extreme relativistic limit, $\varepsilon \gg 1$, H_{DO} can be approximated by the Hamiltonian for a Weyl fermion in a spin-dependent potential, $H_r = c\hat{\sigma}_x\hat{p} - cm\omega\hat{\sigma}_y\hat{x}$, in which case spin-orbit coupling fully dominates the dynamics and renders our measurement scheme meaningless.

Implementation.—The tabletop simulation of relativistic quantum systems has witnessed considerable recent progress. The use of a single trapped ion to simulate the Dirac equation was proposed by Lamata *et al.* [19] and experimentally realized by Gerristma *et al.* [20]. Solano and co-workers [21] demonstrated the mapping of the Dirac oscillator onto the Jaynes-Cummings model. Reference [22] reported the realization of a Dirac oscillator in a microwave system, with further proposals involving fiber Bragg gratings [23], hexagonal structures of

TABLE I. Mapping of key physical quantities of the original Dirac oscillator onto its spin-orbit-coupled condensate implementation, with magnitudes taken from the experiments of Refs. [29,30]. The magnitude of the corresponding parameters for possible circuit-QED and ion implementations are also given for comparison, based on Refs. [19,32].

Dirac oscillator	Electron	SOC condensate	cQED	Ion
Velocity of light (m/s)	$c \sim 10^8$	$\tilde{c} = \hbar k_r/m_a \sim 10^{-2}$	~ 10	$\sim 10^{-3}$
Rest mass (kg)	$m_e \sim 10^{-31}$	$\tilde{m} = \chi m_a^2/\hbar k_r^2 \sim 10^{-27}$	$\sim 10^{-26}$	$\sim 10^{-23}$
Reduced Compton wavelength (m)	$\lambda\!\!\!^{-}_c = \hbar/m_e c \sim 10^{-12}$	$\tilde{\lambda}\!\!\!^{-}_c = \hbar k_r/\chi m_a \sim 10^{-5}$	$\sim 10^{-9}$	$\sim 10^{-8}$
Zitterbewegung frequency ($2\pi \times$ Hz)	$\Omega_{zb} = 2m_e c^2/\hbar \sim 10^{21}$	$\tilde{\Omega}_{zb} = 2\chi \sim 10^3$	$\sim 10^{10}$	$\sim 10^5$
Oscillator frequency ($2\pi \times$ Hz)	ω	$\tilde{\omega} = \hbar k_r \varsigma/m_a \chi \sim 0 - 10^4$	$\sim 10^{10}$	$\sim 10^6$
Relativistic parameter	$\varepsilon = \hbar\omega/m_e c^2$	$\tilde{\varepsilon} = \hbar k_r \varsigma/m_a \chi^2 \sim 0$–$10$	~ 1	~ 10

graphene [24], superconducting qubits [25], and optomechanical arrays [26].

We propose here an alternative scheme based on a spin-orbit coupled (SOC) atomic condensate [27], as its macroscopic coherence provides considerable flexibility toward the realization of measurements spanning a broad parameter range from the effective "nonrelativistic" to a "strongly relativistic" limit. We consider an atomic Bose-Einstein condensate (BEC) of three-level atoms with a pair of pseudospin hyperfine lower states optically coupled by two Raman fields far-off resonant from an upper electronic state that is adiabatically eliminated from the dynamics. The resulting transitions between hyperfine states are accompanied by a momentum transfer of $2\hbar k_r$ in the x direction, where $\hbar k_r$ is the photon recoil momentum. The dynamics in the other two directions are assumed to be decoupled, resulting in an effective one-dimensional situation.

In the mean-field approximation the dynamics of the condensate can be described by a 1D Gross-Pitaevskii equation for the Hamiltonian $H_s + H_c$, where H_s is the single-atom Hamiltonian and H_c accounts for two-body collisions. In momentum representation and the basis of the two hyperfine states H_s is

$$H_s = \begin{pmatrix} \frac{\hbar^2(k+k_r)^2}{2m_a} + \frac{\hbar\delta}{2} & \hbar\Omega \\ \hbar\Omega^* & \frac{\hbar^2(k-k_r)^2}{2m_a} - \frac{\hbar\delta}{2} \end{pmatrix}, \tag{10}$$

where m_a is the atomic mass and δ and Ω are the two-photon detuning and effective Rabi coupling. This is similar to the model describing recent experiments on SOC BEC [28–31], with the difference that we assume that the real part of the two-photon Rabi coupling Ω has a linear spatial dependence, $\Omega = |\Omega| e^{i\phi(x)}$, with $\phi(x)$ slowly varying over the length of the condensate and $\phi(x_0) = \pi/2$ at its center x_0 so that $\Omega(x_0)$ is purely imaginary. This can be achieved by controlling the relative phase of the two Raman fields with a spatial phase modulator. We then have

$$\Omega \approx -\hat{x}|\Omega(x_0)| \left.\frac{\partial\phi(x)}{\partial x}\right|_{x_0} + \Omega(x_0) \equiv -\varsigma\hat{x} + i\chi, \tag{11}$$

where $\chi = \mathrm{Im}[\Omega(x_0)]$. Hence, the real part of the two-photon Rabi frequency has a linear dependence on position, while its imaginary part is constant. With the matrix representation of Pauli operators and after a pseudospin rotation $\sigma_x \to \sigma_y \to \sigma_z \to \sigma_x$, Eqs. (10) and (11) give, for $\delta = 0$ and $k \ll k_r$,

$$H_s = \frac{\hbar^2 k_r^2}{2m_a} + \frac{\hbar^2 k_r}{m_a} k\hat{\sigma}_x - \hbar\varsigma\hat{x}\hat{\sigma}_y + \hbar\chi\hat{\sigma}_z. \tag{12}$$

Except for the kinetic energy term this Hamiltonian has the same form as H_{DO}, with effective mappings between the velocity of light c and the atomic recoil velocity $\hbar k_r/m$, and between the rest energy mc^2 and the Rabi coupling energy $\hbar\chi$. Here, k_r, ς, and $\chi > 0$. Importantly, the kinetic energy term raises up the zero energy level to $\hbar^2 k_r^2/2m_a$, allowing the physical implementation of an analog of negative-energy states. See Table I for the full mapping between the two systems and an estimate of the order of magnitude of the key parameters.

The two-body collisions are described by the Hamiltonian

$$H_c = \begin{pmatrix} g_{\uparrow\uparrow}|\psi_\uparrow|^2 + g_{\uparrow\downarrow}|\psi_\downarrow|^2 & 0 \\ 0 & g_{\uparrow\downarrow}|\psi_\uparrow|^2 + g_{\downarrow\downarrow}|\psi_\downarrow|^2 \end{pmatrix}, \tag{13}$$

where $\psi_{\uparrow,\downarrow}$ are the many-body wave functions for atoms in the spin-up and spin-down hyperfine levels, and $g_{ij} = 4\pi\hbar^2 a_{ij}/m$, with a_{ij} the corresponding scattering lengths, measure the effective inter- and intraspin collision strengths. When collisions dominate, the condensate can be described in a single-mode approximation, as is the case, e.g., for ^{87}Rb, for which $g_{\uparrow\uparrow} = g_{\uparrow\downarrow} \approx g_{\downarrow\downarrow}$ [30]. This results in the effective Hamiltonian

$$\mathcal{H} = \frac{2\tilde{c}}{\hbar}\hat{S}_x\hat{p} - \frac{2\tilde{c}\,\tilde{m}\,\tilde{\omega}}{\hbar}\hat{S}_y\hat{x} + \frac{2\tilde{m}\tilde{c}^2}{\hbar}\hat{S}_z, \tag{14}$$

where $\hat{S}_{x,y,z} = \hbar/2\sum_i^N \hat{\sigma}_{x,y,z}^i$ are collective spin operators with N the number of atoms, and we have neglected

terms proportional to $g_{\uparrow\uparrow}-g_{\downarrow\downarrow}$ and $g_{\uparrow\uparrow}+g_{\downarrow\downarrow}-2g_{\uparrow\downarrow}$. This Hamiltonian has the same form as H_{DO}, with the substitution of $\hat{\sigma}_{x,y,z}$ by $\hat{S}_{x,y,z}$.

The nonrelativistic limit of $\mathcal{H}$ is approached under the strong Raman coupling condition $\chi \gg \sqrt{\hbar k_r \varsigma/m_a}$, resulting in an approximate Hamiltonian

$$\mathcal{H}_{\mathrm{nr}}=\left(2\tilde{m}\tilde{c}^2+\frac{\hat{p}^2}{\tilde{m}}+\tilde{m}\tilde{\omega}^2\hat{x}^2\right)\hat{S}_z/\hbar, \tag{15}$$

which has the same form as Eq. (4), so that the previous discussion can be readily applied [33].

For a measurement interaction of the form

$$\mathcal{V}_{\mathrm{nr}}=Ng\hat{b}^\dagger\hat{b}\,\hat{x}+2f\hat{S}_z\hat{x}/\hbar, \tag{16}$$

the coupling to the perturbation f, of the form $2f\hat{S}_y\hat{x}/\hbar$ in the original physical representation, could be realized through a spatially dependent Raman coupling such that the spatial dependence appears now in the imaginary part of the effective Rabi frequency. The interaction with the measurement apparatus $Ng\hat{x}\hat{b}^\dagger\hat{b}$ can be realized by an optomechanical-like collective coupling between the condensate and a cavity field $\hat{b}$ [34,35]. As with the original Dirac oscillator, the departure from the nonrelativistic regime resulting from a decrease in $\hbar\chi$ results in an increase in backaction, now from the analog of *Zitterbewegung* oscillations [29,36].

In that limit $\mathcal{H}$ simplifies to

$$\mathcal{H}_r=\frac{2\tilde{c}}{\hbar}\hat{S}_x\hat{p}-\frac{2\tilde{c}\,\tilde{m}\,\tilde{\omega}}{\hbar}\hat{S}_y\hat{x}, \tag{17}$$

compare to the Weyl fermion Hamiltonian H_r. For a sufficiently large number of atoms highly polarized along the direction of $\hat{S}_z$, a Holstein-Primakoff transformation is sometimes invoked to map the collective spin operators to position and momentum operators of an effective oscillator, $\hat{x}_s=\hat{S}_y/\sqrt{|S_z|}$, $\hat{p}_s=-\mathrm{sgn}(S_z)\hat{S}_x/\sqrt{|S_z|}$, and $S_z\approx\pm\hbar N/2$ [4] so that

$$\mathcal{H}_r\approx-\tilde{c}\sqrt{2N/\hbar}\,[\mathrm{sgn}(S_z)\hat{p}\hat{p}_s+\tilde{m}\,\tilde{\omega}\,\hat{x}\,\hat{x}_s], \tag{18}$$

with $[\hat{x},\hat{p}_s]=0$. For the coupling $\mathcal{V}_r=Ng\hat{b}^\dagger\hat{b}\,\hat{x}+2f\hat{S}_y/\hbar$, $\hat{x}$ and $\hat{p}_s$ now appear to constitute a true QMFS. However, this relies on neglecting the quantum fluctuations of $\hat{S}_z$, that is, on treating it as a classical quantity. (The same would hold for H_r if $\hat{\sigma}_z$ was treated classically.) But the fundamental reason why a QMFS cannot be realized in the Dirac oscillator is precisely that σ_z is an operator, and that same issue appears in the atomic system as well. In that case, measurement backaction would serve as a probe of the limitations of the Holstein-Primakoff approximation.

Summary and outlook.—Summarizing, we have shown that despite the existence of negative energy states the Dirac oscillator is fundamentally different from a system of two harmonic oscillators with equal and opposite masses, and as a consequence cannot operate as a QMFS backaction evading detector. The origin of this difference is a spin-orbit coupling interaction that results in the relativistic regime in *Zitterbewegung* oscillations. We suggested that measurement backaction can be exploited as a probe of the associated virtual pair creation, and proposed a tabletop demonstration of this effect in a spin-orbit-coupled atomic condensate.

We acknowledge enlightening discussions with J. Chen and W. Xie. Work was supported by the National Key Research and Development Program of China (Grant No. 2016YFA0302001), the National Natural Science Foundation of China (Grants No. 11574086, No. 91436211, No. 11654005, No. 11234003, and No. 11374003), the Shanghai Rising-Star Program (Grant No. 16QA1401600), and the Science and Technology Commission of Shanghai Municipality (Grant No. 16DZ2260200).

*kyzhang@phy.ecnu.edu.cn
†wpz@sjtu.edu.cn

[1] M. Tsang and C. M. Caves, Evading Quantum Mechanics: Engineering a Classical Subsystem within a Quantum Environment, Phys. Rev. X **2**, 031016 (2012).
[2] K. Hammerer, M. Aspelmeyer, E. S. Polzik, and P. Zoller, Establishing Einstein-Poldosky-Rosen Channels between Nanomechanics and Atomic Ensembles, Phys. Rev. Lett. **102**, 020501 (2009).
[3] W. Wasilewski, K. Jensen, H. Krauter, J. J. Renema, M. V. Balabas, and E. S. Polzik, Quantum Noise Limited and Entanglement-Assisted Magnetometry, Phys. Rev. Lett. **104**, 133601 (2010).
[4] C. B. Møller, R. A. Thomas, G. Vasilakis, E. Zeuthen, Y. Tsaturyan, M. Balabas, K. Jensen, A. Schliesser, K. Hammerer, and E. S. Polzik, Quantum back-action-evading measurement of motion in a negative mass reference frame, Nature (London) **547**, 191 (2017).
[5] C. F. Ockeloen-Korppi, E. Damskagg, J. M. Pirkkalainen, A. A. Clerk, M. J. Woolley, and M. A. Sillanpaa, Quantum Backaction Evading Measurement of Collective Mechanical Modes, Phys. Rev. Lett. **117**, 140401 (2016).
[6] K. Zhang, P. Meystre, and W. Zhang, Back-action-free quantum optomechanics with negative-mass Bose-Einstein condensates, Phys. Rev. A **88**, 043632 (2013).
[7] M. Moshinsky and A. Szczepaniak, The Dirac oscillator, J. Phys. A **22**, L817 (1989).
[8] E. Sadurní, The Dirac-Moshinsky oscillator: Theory and applications, AIP Conf. Proc. **1334**, 249 (2011).
[9] C. Quesne, The Dirac oscillator from theory to experiment, J. Phys. A **50**, 081001 (2017).
[10] A. Bermudez, M. A. Martin-Delgado, and A. Luis, Chirality quantum phase transition in the Dirac oscillator, Phys. Rev. A **77**, 063815 (2008).

[11] C. Quimbay and P. Strange, Graphene physics via the Dirac oscillator in $(2+1)$ dimensions, arXiv:1311.2021.
[12] A. Bermudez, M. A. Martin-Delgado, and E. Solano, Mesoscopic Superposition States in Relativistic Landau Levels, Phys. Rev. Lett. **99**, 123602 (2007).
[13] P. Rozmej and R. Arvieu, The Dirac oscillator. A relativistic version of the Jaynes-Cummings model, J. Phys. A **32**, 5367 (1999).
[14] If the external perturbation f is spin independent then for a spin-dependent phase imprinting, we can obtain similar dynamical equations for $\hat{\Phi}$ and $\hat{P}$.
[15] A Foldy-Wouthuysen transformation could be performed to formally eliminate the *Zitterbewegung*. However, for that case the quantity to be measured is the Newton-Wigner position, which is not diagonal in coordinate space and would require a more complex measurement method. See Supplemental Material at http://link.aps.org/supplemental/10.1103/PhysRevLett.121.110401 for a detailed discussion, which includes Refs. [16,17].
[16] M. Moreno and A. Zentella, Covariance, *CPT* and the Foldy-Wouthuysen transformation for the Dirac oscillator, J. Phys. A **22**, L821 (1989).
[17] F. M. Toyama, Y. Nogami, and F. A. B. Coutinho, Behaviour of wavepackets of the "Dirac oscillator": Dirac representation versus Foldy-Wouthuysen representation, J. Phys. A **30**, 2585 (1997).
[18] W. Greiner, *Relativistic Quantum Mechanics: Wave Equations* (Springer-Verlag, Berlin, Heidelberg, 2000).
[19] L. Lamata, J. León, T. Schätz, and E. Solano, Dirac Equation and Quantum Relativistic Effects in a Single Trapped Ion, Phys. Rev. Lett. **98**, 253005 (2007).
[20] R. Gerritsma, G. Kirchmair, F. Zähringer, E. Solano, R. Blatt, and C. F. Roos, Quantum simulation of the Dirac equation, Nature (London) **463**, 68 (2010).
[21] A. Bermudez, M. A. Martin-Delgado, and E. Solano, Exact mapping of the $2+1$ Dirac oscillator onto the Jaynes-Cummings model: Ion-trap experimental proposal, Phys. Rev. A **76**, 041801 (2007).
[22] J. A. Franco-Villafañe, E. Sadurní, S. Barkhofen, U. Kuhl, F. Mortessagne, and T. H. Seligman, First Experimental Realization of the Dirac Oscillator, Phys. Rev. Lett. **111**, 170405 (2013).
[23] S. Longhi, Photonic realization of the relativistic Dirac oscillator, Opt. Lett. **35**, 1302 (2010).
[24] E. Sadurní, T. H. Seligman, and F. Mortessagne, Playing relativistic billiards beyond graphene, New J. Phys. **12**, 053014 (2010).
[25] J. S. Pedernales, R. Di Candia, D. Ballester, and E. Solano, Quantum simulations of relativistic quantum physics in circuit QED, New J. Phys. **15**, 055008 (2013).
[26] M. Schmidt, V. Peano, and F. Marquardt, Optomechanical Dirac physics, New J. Phys. **17**, 023025 (2015).
[27] Y. J. Lin, K. Jiménez-García, and I. B. Spielman, Spin-orbit-coupled Bose-Einstein condensates, Nature (London) **471**, 83 (2011).
[28] J. Y. Zhang *et al.*, Collective Dipole Oscillations of a Spin-Orbit Coupled Bose-Einstein Condensate, Phys. Rev. Lett. **109**, 115301 (2012).
[29] L. J. LeBlanc, M. C. Beeler, K. Jiménez-García, A. R. Perry, S. Sugawa, R. A. Williams, and I. B. Spielman, Direct observation of *Zitterbewegung* in a Bose-Einstein condensate, New J. Phys. **15**, 073011 (2013).
[30] C. Hamner, C. Qu, Y. Zhang, J. Chang, M. Gong, C. Zhang, and P. Engels, Dicke-type phase transition in a spin-orbit-coupled Bose-Einstein condensate, Nat. Commun. **5**, 4023 (2014).
[31] J.-R. Li, J. Lee, W. Huang, S. Burchesky, B. Shteynas, F. Ç. Top, A. O. Jamison, and W. Ketterle, A stripe phase with supersolid properties in spin-orbit-coupled Bose-Einstein condensates, Nature (London) **543**, 91 (2017).
[32] A. Blais, R. Huang, A. Wallraff, S. M. Girvin, and R. J. Schoelkopf, Cavity quantum electrodynamics for superconducting electrical circuits: An architecture for quantum computation, Phys. Rev. A **69**, 062320 (2004).
[33] Remember, however, that a pseudospin rotation was applied in the derivation of H_s, see Eq. (12); this means that the initial atomic states must satisfy the condition $\langle \hat{S}_y \rangle = 0$ in the original physical representation.
[34] F. Brennecke, S. Ritter, T. Donner, and T. Esslinger, Cavity optomechanics with a Bose-Einstein condensate, Science **322**, 235 (2008).
[35] K. W. Murch, K. L. Moore, S. Gupta, and D. M. Stamper-Kurn, Observation of quantum-measurement backaction with an ultracold atomic gas, Nat. Phys. **4**, 561 (2008).
[36] J. Vaishnav and C. Clark, Observing *Zitterbewegung* with Ultracold Atoms, Phys. Rev. Lett. **100**, 153002 (2008).